

A new crystalline phase of nitric acid dihydrate

Nathalie Lebrun,^{a*} Fabrice Mahe,^b Jocelyne Lamiot,^a
Michel Foulon^a and Jean Claude Petit^b

^aLaboratoire de Dynamique et Structure des Matériaux Moléculaires (ESA 8024), UFR de Physique, Bâtiment P5, 59655 Villeneuve d'Ascq Cedex, France, and ^bLaboratoire de Combustion et Systèmes Réactifs, CNRS, 1c Avenue de la Recherche Scientifique, 45071 Orléans, France

Correspondence e-mail: nathalie.lebrun@univ-lille1.fr

Received 13 June 2001

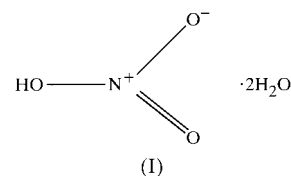
Accepted 18 June 2001

The crystal structure of a new high-temperature phase of nitric acid dihydrate, $\text{HNO}_3 \cdot 2\text{H}_2\text{O}$, has been determined at 225 K by single-crystal X-ray diffraction. The H atom of the nitric acid is delocalized to one water molecule, leading to an association of equimolar NO_3^- and H_3O^+ ionic groups. The asymmetric unit contains two molecules of $\text{HNO}_3 \cdot 2\text{H}_2\text{O}$. The two independent molecules are related by a pseudo-twofold c axis, by a translation of 0.54 (approximately $\frac{1}{2}$) along \mathbf{b} , with a mean atomic distance difference of 0.3 Å, except for one H atom of the water molecules (1.5 Å), because of their different orientations in the two molecules. The two independent molecules, linked by strong hydrogen bonds, are arranged in layers. These layers are linked by weaker hydrogen bonds oriented approximately along the c axis. A three-dimensional hydrogen-bond network is observed.

Comment

It is known that polar stratospheric aerosols play a crucial role in ozone depletion in Arctic and Antarctic regions (Solomon, 1988). Heterogeneous processes which occur at the surface of these aerosols lead to the easy formation of chlorine radicals (Cl and ClO), resulting in catalytic ozone destruction. The reaction mechanism remains controversial, due to the lack of information on the physical state of some hydrates of nitric and sulfuric acids. Previous experimental reports indicated the possible crystallization of the dihydrate of nitric acid, denoted NAD (Ji & Petit, 1991, 1993). Recent powder and single-crystal X-ray diffraction experiments (Lebrun *et al.*, 2001) confirmed the formation of NAD and identified one stable crystalline phase, denoted NAD(I), at low temperature. Under particular thermal conditions, the crystallization of a new polymorphic phase, denoted NAD(II) and never previously observed, was revealed (Mahe, 1999). NAD(II) transforms at 235 K, on heating, into nitric acid trihydrate, denoted NAT, via a peritectic reaction: $\text{NAD(II)} \rightarrow \text{liquid} + \text{NAT}$ (Mahe *et al.*, 2000).

As for NAD(I), the solid phase of NAD(II) crystallizes in space group $P2_1/n$ with two independent molecules, denoted A and B , in the asymmetric unit. These molecules are arranged in planes linked together by hydrogen bonds. One layer of molecules is shown in Fig. 1 and selected geometric parameters are given in Table 1.



The delocalization of the nitric acid H atom to one water molecule leads to the formation of a nitrate ion, NO_3^- , an oxonium ion, H_3O^+ , and a water molecule, all three moieties being linked together by strong hydrogen bonds. In each independent molecule, the oxonium ion is strongly linked, *via* one H atom (H2A or H2B), to the water molecule involving the acceptor O atom (O5A or O5B), leading to an unsymmetrical H_5O_2^+ ion. The mean values of these 'intramolecular' hydrogen bonds are $\text{O} \cdots \text{O} = 2.51 \text{ \AA}$, $\text{O} \cdots \text{H} = 1.63 \text{ \AA}$ and $\text{O}-\text{H} \cdots \text{O} = 176^\circ$. The oxonium ion is also linked to the nitrate ion *via* weaker hydrogen bonds ($\text{O}2\text{A} \cdots \text{H}3\text{A}-\text{O}4\text{A}$ and $\text{O}2\text{B} \cdots \text{H}3\text{B}-\text{O}4\text{B}$), with mean values of $\text{O} \cdots \text{O} = 2.64 \text{ \AA}$, $\text{O} \cdots \text{H} = 1.87 \text{ \AA}$ and $\text{O}-\text{H} \cdots \text{O} = 175^\circ$. The hydrogen-bonding geometry is reported in Table 2. Only two O atoms of the NO_3^- ions are engaged in three acceptor hydrogen bonds (see Fig. 1), explaining the significantly shorter length observed for one N—O bond (NA—O3A and NB—O3B).

The two independent molecules, A and B , are related by a pseudo-twofold c axis, with a translation of 0.54 (approximately $\frac{1}{2}$) along the b axis. Applying this pseudosymmetry to molecule B , the mean distance between the corresponding atoms is low (0.3 Å), except for the water molecules (1.5 Å between H5A and H5B), because of their different orienta-

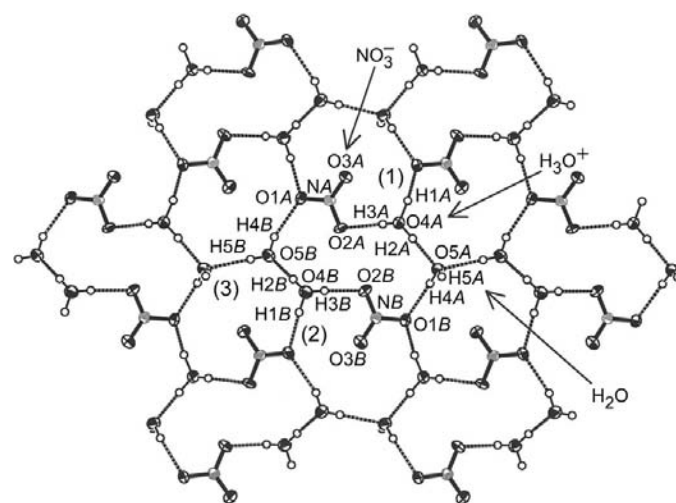


Figure 1
Projection along [001] of the two independent molecules of NAD, A and B , showing their neighbourhood in one layer ($L1$ plane) and the atom-numbering scheme. Hydrogen bonds are indicated by thin broken lines and displacement ellipsoids are drawn at the 50% probability level.

tions, as shown in Fig. 1. Molecules *A* and *B* are linked together by weak $O1A \cdots H4B - O5B$ and $O1B \cdots H4A - O5A$ hydrogen bonds. The mean values of these hydrogen bonds are $O \cdots O = 2.83 \text{ \AA}$, $O \cdots H = 2.02 \text{ \AA}$ and $O - H \cdots O = 161^\circ$.

In one plane, the molecular groups formed by molecules *A* and *B* are related by a diagonal symmetry plane. Each group is linked to six other neighbouring groups *via* three different hydrogen bonds, denoted (1) $O4A - H1A \cdots O1B^{ii}$, (2) $O4B - H1B \cdots O1A^i$ and (3) $O5B - H5B \cdots O5A^{iii}$, leading to a complicated two-dimensional hydrogen-bond network, as shown in Fig. 1 [symmetry codes: (i) $-\frac{1}{2} - x, y - \frac{1}{2}, \frac{1}{2} - z$; (ii) $\frac{1}{2} - x, \frac{1}{2} + y, \frac{1}{2} - z$; (iii) $x - 1, y, z$].

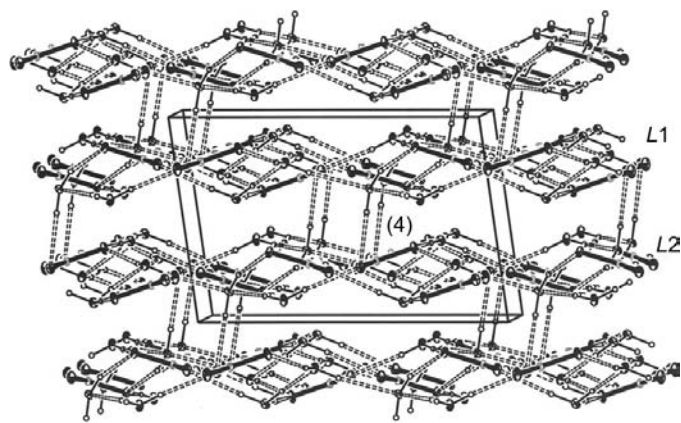


Figure 2
The projection of NAD along the [010] direction, showing the two types of layers (*L1* and *L2*) and the crystal packing.

A perspective view of the structure, nearly parallel to the *b* axis, is shown in Fig. 2. The structure may be described by two different planes, *L1* and *L2*, spaced by *c*/2 and parallel to the *ab* plane. *L2* is deduced from *L1* by inversion symmetry. These layers are weakly linked by one type of hydrogen bond, denoted (4) in Fig. 2, involving the 'out of layer' H atom, H5A, of the water molecule in layer *L1* as donor to the nitrate ion of molecule *A* located in layer *L2*. The structure may be described by the translation of this group of two linked layers along the [001] direction, leading to a complex three-dimensional hydrogen-bond network.

Experimental

Despite numerous attempts with the NAD composition $X(\text{HNO}_3) = 0.33$, no single crystal of NAD(II) was obtained *in situ* on the four-circle diffractometer. The adapted Bridgman method used at this composition was not successful, since NAD(II) always transformed at 235 K into NAT + liquid. According to the phase diagram established by Ji & Petit (1991, 1993) and Mahe (1999), a composition near the eutectic liquid \rightarrow NAT + NAD [$X(\text{HNO}_3) = 0.38$] (NAT is nitric acid monohydrate) was chosen, since the kinetics of crystallization of NAT and NAD are slower than those observed at $X(\text{HNO}_3) = 0.33$. The liquid was enclosed in a sharpened Lindemann tube. Thermal treatment was carried out using a low-temperature nitrogen gas flow device. The liquid [$X(\text{HNO}_3) = 0.38$] was cooled rapidly from 293 to 183 K and crystallized into the NAD(I) form, with liquid remaining.

After a rapid increase of the temperature to 200 K, the solid was heated slowly to 225 K and the transition NAD(I) \rightarrow NAD(II) was observed at 210 K. At 225 K, a mixture of the two solids was obtained, *i.e.* large single-crystal domains of NAD(II) surrounded by crystalline solids of NAT, as provided by the binary phase diagram for $\text{HNO}_3 \cdot \text{H}_2\text{O}$ (Ji & Petit, 1991, 1993). A large single-crystal domain of NAD(II) of sufficiently good quality was selected and data collection was possible in the range $\theta = 2\text{--}20^\circ$. The low-temperature nitrogen gas flow failed before the end of the data collection, so that only 467 unique reflections were measured instead of the expected 756. Other attempts at single-crystal growth were carried out without success. During data collection, three reflections were measured every 60 min. These reference intensities increased linearly (13.2, 9.7 and 12.1%, respectively), probably due to some molecular rearrangement of the single crystal. An averaged correction was applied to the diffracted intensities.

Crystal data

$\text{HNO}_3 \cdot 2\text{H}_2\text{O}$	$D_x = 1.638 \text{ Mg m}^{-3}$
$M_r = 99.05$	Mo $K\alpha$ radiation
Monoclinic, $P2_1/n$	Cell parameters from 25 reflections
$a = 9.674 (3) \text{ \AA}$	$\theta = 3\text{--}8^\circ$
$b = 12.920 (4) \text{ \AA}$	$\mu = 0.19 \text{ mm}^{-1}$
$c = 6.484 (3) \text{ \AA}$	$T = 225 \text{ K}$
$\beta = 97.71 (3)^\circ$	Cylindrical, colourless
$V = 803 (1) \text{ \AA}^3$	Crystal size: unknown
$Z = 8$	

Data collection

Philips PW1100 four-circle diffractometer	$h = -9 \rightarrow 9$
$\omega/2\theta$ scans	$k = 0 \rightarrow 12$
503 measured reflections	$l = 0 \rightarrow 6$
467 independent reflections	3 standard reflections
414 reflections with $I > 3\sigma(I)$	frequency: 60 min
$\theta_{\text{max}} = 20^\circ$	intensity decay: 11.5%

Refinement

Refinement on F^2	$w = 1/[\sigma^2(F_o^2) + (0.0617P)^2]$
$R(F) = 0.031$	where $P = (F_o^2 + 2F_c^2)/3$
$wR(F^2) = 0.083$	$(\Delta/\sigma)_{\text{max}} = 0.001$
$S = 1.12$	$\Delta\rho_{\text{max}} = 0.14 \text{ e \AA}^{-3}$
414 reflections	$\Delta\rho_{\text{min}} = -0.15 \text{ e \AA}^{-3}$
140 parameters	Extinction correction: SHELXL93 (Sheldrick, 1993)
All H-atom parameters refined	Extinction coefficient: 0.009 (3)

Table 1

Selected geometric parameters (\AA , $^\circ$).

NA—O1A	1.263 (4)	NB—O1B	1.278 (4)
NA—O2A	1.265 (4)	NB—O2B	1.246 (4)
NA—O3A	1.214 (4)	NB—O3B	1.227 (4)
O2A—NA—O3A	121.2 (3)	O2B—NB—O3B	122.0 (3)
O2A—NA—O1A	117.9 (3)	O2B—NB—O1B	117.8 (3)
O3A—NA—O1A	120.9 (3)	O3B—NB—O1B	120.1 (3)
H3A—O4A—H1A	111 (3)	H3B—O4B—H2B	114 (3)
H3A—O4A—H2A	117 (3)	H3B—O4B—H1B	109 (3)
H1A—O4A—H2A	114 (3)	H2B—O4B—H1B	109 (3)
H5A—O5A—H4A	114 (3)	H4B—O5B—H5B	117 (3)

Despite the low number of unique measured reflections and the poor quality of the crystal, the refinement led to a good reliability factor (3.08%) with 140 refined parameters. The H atoms were located on a difference Fourier map. During the refinement procedures, short hydrogen-bond lengths were found for the oxonium ion

Table 2

Hydrogen-bonding geometry (Å, °).

<i>D</i> —H... <i>A</i>	<i>D</i> —H	H... <i>A</i>	<i>D</i> ... <i>A</i>	<i>D</i> —H... <i>A</i>
O5 <i>B</i> —H4 <i>B</i> ...O1 <i>A</i>	0.83 (3)	2.04 (5)	2.832 (4)	159 (5)
O5 <i>A</i> —H4 <i>A</i> ...O1 <i>B</i>	0.86 (4)	2.00 (6)	2.827 (4)	162 (7)
O4 <i>A</i> —H3 <i>A</i> ...O2 <i>A</i>	0.75 (5)	1.88 (5)	2.626 (4)	176 (4)
O4 <i>B</i> —H3 <i>B</i> ...O2 <i>B</i>	0.82 (3)	1.85 (4)	2.663 (4)	175 (5)
O4 <i>B</i> —H2 <i>B</i> ...O5 <i>B</i>	0.89 (3)	1.57 (4)	2.459 (4)	178 (5)
O4 <i>A</i> —H2 <i>A</i> ...O5 <i>A</i>	0.88 (5)	1.68 (4)	2.553 (5)	175 (4)
O4 <i>B</i> —H1 <i>B</i> ...O1 <i>A</i> ⁱ	0.89 (3)	1.75 (4)	2.640 (4)	177 (4)
O4 <i>A</i> —H1 <i>A</i> ...O1 <i>B</i> ⁱⁱ	1.00 (5)	1.53 (5)	2.522 (5)	171 (5)
O5 <i>B</i> —H5 <i>B</i> ...O5 <i>A</i> ⁱⁱⁱ	0.82 (3)	1.98 (5)	2.800 (4)	173 (6)
O5 <i>A</i> ⁱⁱ —H5 <i>A</i> ⁱⁱ ...O2 <i>A</i> ^{iv}	0.80 (3)	2.10 (5)	2.884 (5)	167 (5)

Symmetry codes: (i) $-\frac{1}{2} - x, y - \frac{1}{2}, \frac{1}{2} - z$; (ii) $\frac{1}{2} - x, \frac{1}{2} + y, \frac{1}{2} - z$; (iii) $x - 1, y, z$; (iv) $-x, 1 - y, -z$.

of molecule *A*. Consequently, the structure was refined with the O4*B*—H1*B*, O4*B*—H2*B* and O4*B*—H3*B* hydrogen-bond lengths constrained between 0.8 and 1.0 Å.

Data collection: *PW1100 Software* (Philips, 1997); cell refinement: *PW1100 Software*; data reduction: *PW1100 Software*; program(s) used to solve structure: *SHELXS86* (Sheldrick, 1985); program(s)

used to refine structure: *SHELXL93* (Sheldrick, 1993); molecular graphics: *ORTEPIII* (Burnett & Johnson, 1996).

Supplementary data for this paper are available from the IUCr electronic archives (Reference: SK1488). Services for accessing these data are described at the back of the journal.

References

- Burnett, M. N. & Johnson, C. K. (1996). *ORTEPIII*. Report ORNL-6895. Oak Ridge National Laboratory, Tennessee, USA.
- Ji, K. & Petit, J. C. (1991). *Air Pollut. Res. Rep.* **42**, 162–165.
- Ji, K. & Petit, J. C. (1993). *C. R. Acad. Sci. Ser. B*, **316-II**, 1743–1748.
- Lebrun, N., Mahe, F., Lamiot, J., Foulon, M., Petit, J. C. & Prevost, D. (2001). *Acta Cryst.* **B57**, 27–35.
- Mahe, F. (1999). Thesis (12/1999), University of Orléans, France.
- Mahe, F., Lebrun, N., Foulon, M., Lamiot, J., Petit, J. C. & Prevost, D. (2000). 26èmes Journées d'Etudes des Equilibres entre Phases (JEEP), Marseille, France, 23–24 March, pp. 16–19.
- Philips (1997). *PW1100 Software*. Version 5. Philips BV, Eindhoven, The Netherlands.
- Sheldrick, G. M. (1985). *SHELXS86*. University of Göttingen, Germany.
- Sheldrick, G. M. (1993). *SHELXL93*. University of Göttingen, Germany.
- Solomon, S. (1988). *Rev. Geophys.* **26**, 131–148.